Sea Level Tidal Attributes in Port Said Harbor, Eastern Egyptian Mediterranean Coast

Mohamed Helmy[1], Ahmed Khedr[2]

Observed sea level data attained from a pressure sensor tide gauge, installed inside Port Said harbor in Egypt, was utilized to modernize tidal characteristics and surges in the study area. Five years of hourly sea level dataset (June 2010 to June 2015) were analyzed using the harmonic analysis approach of Delft-3D Tide suit. The results of the analysis revealed that the semi-diurnal constituents (M2, S2), together with the solar annual (Sa) dominate tide behavior in the area. Furthermore, a semidiurnal tidal regime by a ratio of 0.21 is based on the form factor (FF) equation. Moreover, tidal asymmetry (Ar.) shows a flood tide with a short period of a value equal to 0.01068 > 0.01, which reflects a tide wave distortion. From power spectral analysis, the sea-level change is controlled by both the significant tidal and non-tidal (storm surge) components by almost an equal percentage of 50.63 % and 49.37 % respectively. Additionally, the residual from sea level harmonic analysis was annually correlated with the meteorological parameters of wind, temperature, and atmospheric pressure to estimate their effect on Sea-Level Rise (SLR). A small positive trend line of SL was distinguished in the years from 2011 to 2015 by approximately (2 mm/yr.) due to the weak correlation of meteorological parameters, in conjunction with a conventional relationship with atmospheric pressure and temperature. In 2010, a slight negative linear tendency was noticed of 0.3 mm/yr., which can be related to the direct proportional relation of atmospheric pressure and surge component, besides an inversely proportional relation of air temperature and residual component, regardless of the weak correlation with wind vector. Overall, the research provides insights into the tidal characteristics, surges, and sea-level rise in Port Said Harbor. Understanding these attributes serves the objective of this paper to assess the impact of sea-level rise and develop appropriate adaptation strategies in coastal areas.

[1] University of Benha, Faculty of Engineering, Civil Engineering Department, Benha, Qalyubia, Egypt
University of Bologna, Department of Civil, Chemical, Environmental and Materials Engineering, Bologna, Italy
University of Rome - DICEA-Sapienza, Geodesy and Geomatics Division, Rome, Italy
[2] Arab Academy for Science, College of Maritime Transport and Technology, Abu-Qir, Alexandria, Egypt
e-mail: mohamed.mohsen@bhit.bu.edu.eg
doi: 10.7225/toms.v13.n02.w04

1. INTRODUCTION

The eastern Egyptian coast extends for 455 km between Abu-Qir Bay and El-Arish as shown in Figure (1). Port Said harbor is the main controlling harbor located on the northern tip of the Suez Canal. In addition, it is one of the major harbors along the Egyptian Mediterranean coast (Mackie et al., 2021). This harbor consists of two single-lane waterways with a surface area of about 0.27 km^2 (Biton, 2020). Moreover, it is considered the linking point of the Mediterranean Sea to the Suez Canal. It was established at the time of the Suez Canal excavation in 1869, for the reason of ship services, goods and cargo handling as well as passenger transportation. Sea level is a critical oceanographic parameter that must be taken into consideration and studied carefully to account for regional and global Sea-Level Rise (SLR).

In 1984, Tetra Tech deduced that the tidal regime along the coast of the Nile delta in the Mediterranean Sea was semidiurnal, with the mean and extreme ranges of tide of 17 and 118 cm, respectively. Sharaf El Din *et al*. (1989) analyzed the sea level off Port Said over 49 years, from 1924 to 1976, and found that the mean sea level (MSL) was 49.6 cm above the Egyptian survey zero level (ESA, 1906). El Fishawi (1993) reported a positive trend of the sea level in Port Said by 1.3 mm/year during the period from 1926 to1987. Tsimplis *et al.* (1995) reported that the M2 tidal constituent in the Mediterranean generally had an amplitude of less than 10 cm, with exceptions in specific locations such as the Gulf of Gabes, the northern Aegean Sea, and the northern Egyptian coasts. However, it is the residual elevations, which represent the discrepancy between the recorded sea level and tidal elevations, which play a significant role in the observed fluctuations of sea level along the Egyptian Mediterranean coastline. These residual elevations can reach heights of up to 1.0 m, primarily influenced by atmospheric parameters, as highlighted by El-Geziry and Radwan (2012). Tsimplis and Rixen (2002) stated that the Mediterranean Sea level variability is significantly dominated by the steric effects. A positive sea level trend during the 21st century in the southeastern part of the Mediterranean is expected. This may expose low areas along the Nile Delta coast to inundation (Cazenav *et al*., 2001; IPCC, 2007). Sea-level rise (SLR) can brutally distress coastal properties and lives (Douglas, 2001). The SLR rates fluctuated along the Egyptian Mediterranean Coast between 2.0 and 3.0 mm/yr over different time spans at different locations (El-Geziry and Said, 2019; Hendy *et al*., 2021). El-Geziry and Said (2020) conducted a study and determined that the rate of sea-level rise (SLR) along the Egyptian Mediterranean coastline was 3.4 mm/year. This finding highlights the high vulnerability of the region to the issue of SLR. In a separate study, Syvitski *et al.* (2009) classified the Nile and Niger Deltas as the most vulnerable among the African deltas due to factors such as land subsidence and human activities. El-Geziry (2020) further contributed to the understanding of SLR vulnerability by creating a map specifically for the Egyptian Mediterranean coastline. The map identified different levels of vulnerability across various sections of the coast. The western section, which includes the City of Mersa Matruh, was classified as highly vulnerable to SLR. The northwest section of the Nile Delta, encompassing the Sidi Abdel-Rahman Resort area, was categorized as moderately vulnerable.

On the other hand, the central and northeast sectors of the Nile Delta, which include Alexandria and Port Said, were classified as very highly vulnerable to SLR. These studies provide valuable insights into the vulnerability of the Egyptian Mediterranean coastline to sea-level rise, with specific areas identified as being at higher risk. The findings emphasize the need for effective coastal management strategies and adaptation measures to mitigate the potential impacts of SLR in these vulnerable regions. Due to the importance of the area, sea level rise and tidal characteristics were studied, using hourly sea-level dataset in the period from June 2010 to June 2015, recorded by a tide gauge fixed inside the basin of Port Said harbor, as shown in Figure (1).

Figure 1. Satellite image (Google Earth) of the southeastern Mediterranean Sea and Port Said harbor illustrated on SC-1 Nautical Chart (INT Chart 7159, 2015).

2. DATA COLLECTION AND METHODS OF ANALYSIS

2.1. Types of data

2.1.1. Sea level data

Five years of hourly sea level dataset recorded using tide-gauge (T.G) pressure sensor as shown in Figure 2 was utilized for tidal characteristics calculation. T.G is fixed inside the basin of Port Said (PS) harbor, at the northern tip of the Suez Canal, in the geographical position (31° 16′ N, 32 ° 19 ′ E) and an elevation of 18.047 m above the Egyptian Surveying Authority Datum (ESA zero level).
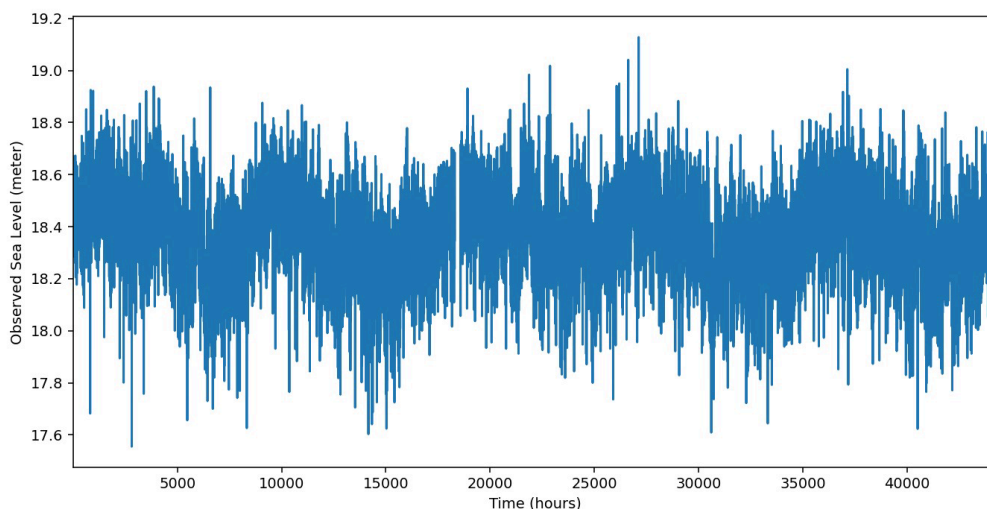

Figure 2. Hourly recorded sea-level data in Port Said harbor, from 23 June 2010 to 14 July 2015.

2.1.2. Meteorological parameters

Five years of hourly meteorological data (atmospheric pressure - air temperature - wind data) was obtained from the automated weather station located in the geographical position (31° 15′ N, 32 ° 18′ E), as shown in Figures 3a – 3c.

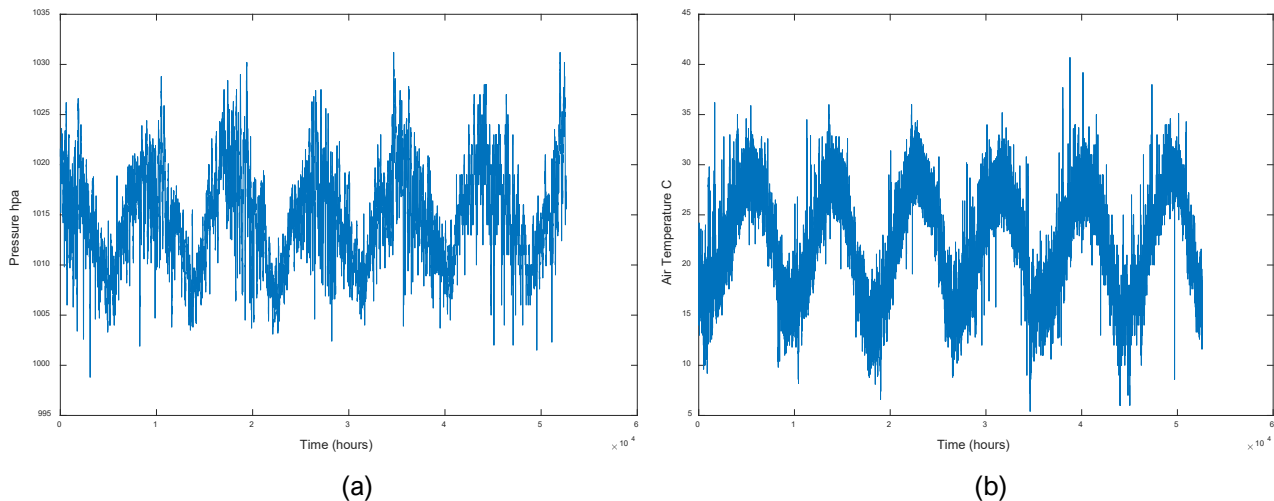(a)   (b)

Figure 3. (a) Observed atmospheric pressure from 1 June 2010 to 12 December 2015; (b) Observed air temperature from 1 June 2010 to 12 December 2015
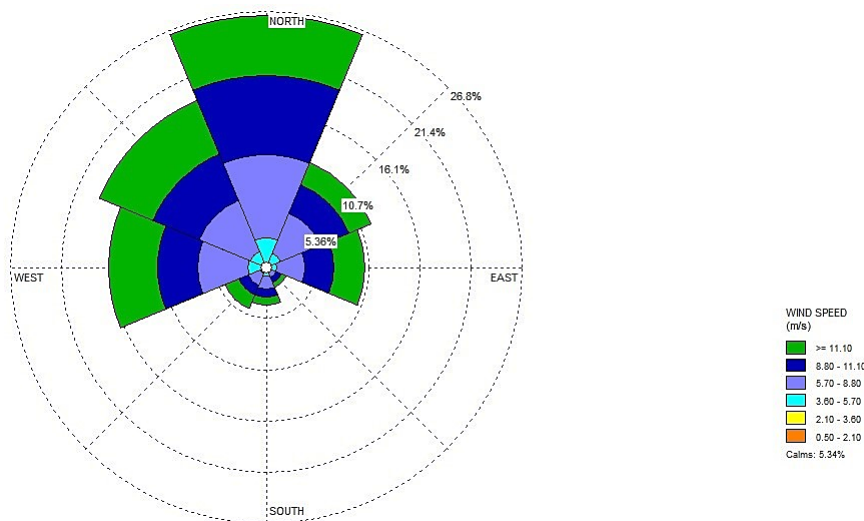

Figure 3c. Wind rose for observed wind data from 1 June 2010 to 12 December 2015

2.2. Methods of analysis

2.2.1. Data preparation

The mean sea level was removed from the observed sea-level in Figure 2; all datasets were free of minor gaps and were categorized and examined for spikes, outliers, and unreliable data readings to be removed from the analysis, as shown in Figures 4a – 4c.
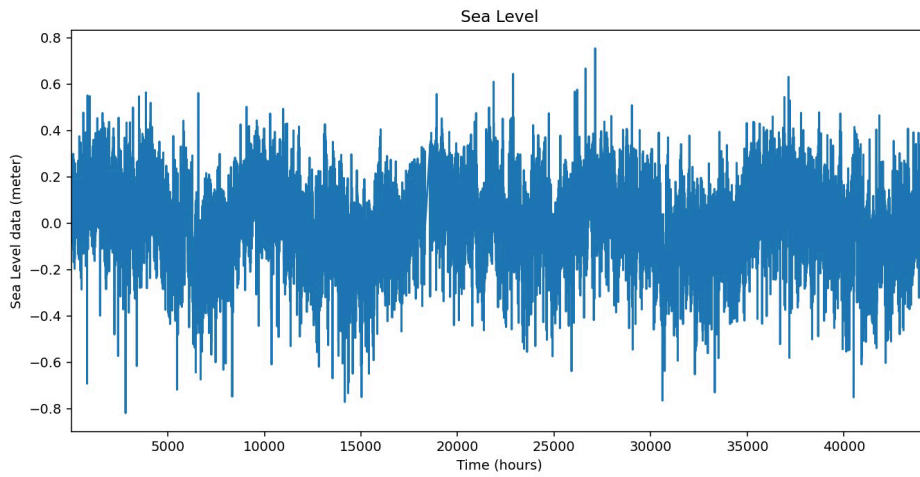
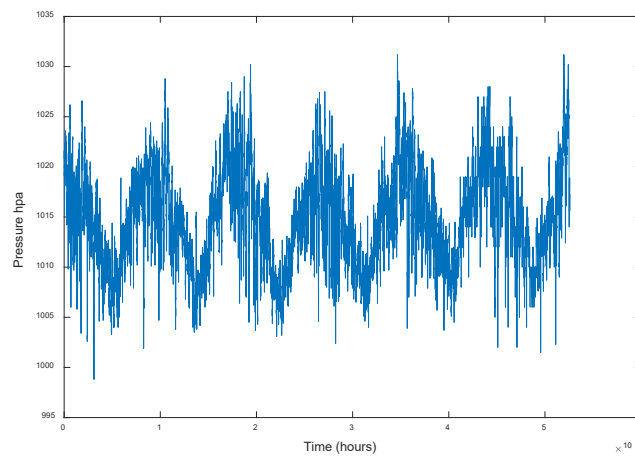Figure 4a. Smoothed observed sea level dataset from 23 June 2010 to 22 June 2015

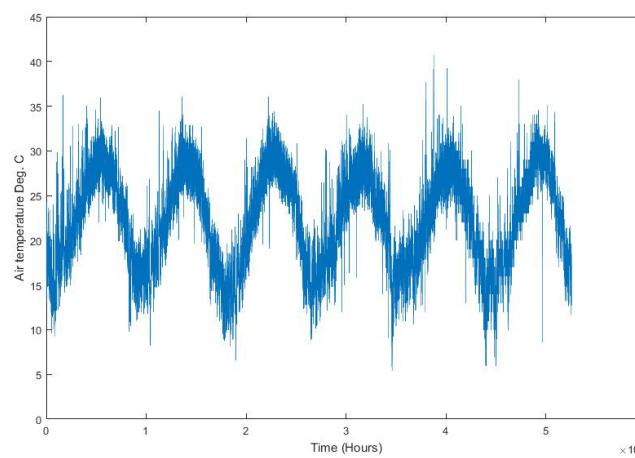Figure 4b. Smoothed observed atmospheric pressure from 23 June 2010 to 22 June 2015

Figure 4c. Smoothed observed air temperature from 23 June 2010 to 22 June 2015

2.2.2. Harmonic analysis

Harmonic analysis is defined as a mathematical analytical process used for extracting frequencies of all known tidal constituents one at a time (Pawlowicz *et al*., 2002). Delft-3D tide suit as one of the powerful tools for analysis was used to obtain tidal constituent amplitudes (Amp.) and phases (phs.). Data input files were prepared in the form of Notepad files using Microsoft Excel as follows:

1) Observed sea level data file arranged in a matrix of 6 columns;
2) Information and input file about analysis criteria and station by which the analysis is performed, such as start and end time, date, total numbers and names of constituents, number of sensors.

Selection of the significant tidal constituents started by choosing 234 available constituents, and then proceeding to the analysis. According to Rayleigh Criterion (ω), which is the minimum frequency between any two neighboring tidal components expressed in degrees per hour that separates any two adjacent tidal constituents, the neighboring tidal constituents was eliminated until it gave a proper representation of the tide in the area by about 71 significant tidal constituents, which reflects the most significant tidal constituents in the area from the previous studies.

2.2.3. Sea-level rise trend

Sea level variations as a very critical matter these days, due to its great influence on coastal cities and harbors. It can be related to many different factors such as: steric effects, global warming and ice melting, or any other meteorological parameters.

- Air temperature is a very important element responsible for global warming and, consequently, ice melting, which leads to the Sea-Level Rise (SLR).
- Atmospheric pressure is considered a regional parameter affecting the SLR with an inversely proportional relation.

Correlation analysis technique was annually applied to define the relations of surge to each parameter independently; therefore, the trend line of sea level is considered as rising or falling (Tonbol and Shaltout, 2013).

2.2.4. Form factor

The area of study has been classified after analyzing the main significant diurnal and semidiurnal constituents (O1, K1, M2, and S2) by form-factor (FF) ratio equation, which is a ratio of amplitudes between the diurnal and semidiurnal, as shown in Eq. (1).

$$F = \frac{H_{O1}+H_{K1}}{H_{M2}+H_{S2}} \qquad (1)$$

Where HO1 is the amplitude of the principal lunar diurnal constituent, HK1 is the amplitude of the luni-solar diurnal constituent, HM2 is the amplitude of the principal lunar semidiurnal constituent, and HS2 is the amplitude of the principal solar semidiurnal constituent.

The value of FF categorized the type of tide into four categories (Pugh, 1987, 2004); the higher the FF is, the more dominant of diurnal type cycle it is. FF is represented by a semidiurnal signal if it is lower than 0.25; from 0.25 to 1.5 it is considered mixed semidiurnal, or a mixed diurnal if it ranged between 1.5 to 3, and a diurnal signal if it was higher than 3.

2.2.5. Tide asymmetry

Nonlinear propagation tide is considered the major effect of asymmetry of the tide. It is described as the bias in a tidal wave. M2 (a principal lunar semidiurnal constituent), is the dominant constituent, along with M4 generated mainly by nonlinear interactions, and other harmonics of higher order are responsible for the tide wave distortion. Nevertheless, M4 is the main contributor to the distortion of tides in the coastal areas.

Asymmetry of the tide is often described by the difference or relationship between the duration of the rising tide (flood) and the falling tide (ebb). If the flood period is shorter, the asymmetry of the vertical tide is flood-dominant. If the ebb period is shorter, the asymmetry is ebb-dominant (Riding and Rawson, 2015). The reasoning behind this is that a shorter flood duration implies stronger flood velocities (peak) and, therefore, higher transport rates in the flood direction, or vice versa. Asymmetry can be calculated using the ratio of M4 and M2 to express the distortion degree using Eq. (2), where Ar is the amplitude ratio. Ar M4 > 0.01 indicates a significant distortion in the tide wave (Dias *et al.,* 2013; Stark *et al*., 2017). The duration of the tide was calculated using Eq. (3).

$$\text{Ar M4} = \frac{\text{M4amp}}{\text{M2amp}} \qquad (2)$$

$$\text{ØM4} = 2\theta\text{M2} - \theta\text{M4} \qquad (3)$$

Where θ shows the phase, and ØM4 indicates the duration of the tide. If the value of ØM4 ranged from 0° to 180°, it indicates a short flood period and the tide is flood-dominant, while if ØM4 ranged from 180° to 360°, the tidal wave is classified as ebb dominant. By this definition, the sediment transport direction can be well defined inside the area (Dias *et al*., 2013; Stark *et al.,* 2017).

2.2.6. Energy percentages of tidal and non-tidal signals

Energy percentages identify the energy contribution of each of the tidal and non-tidal components to the original sea-level signal. It is calculated using MATLAB code and represented by amplitude percentage for each compared to the original signal. Eq. (4) and Eq. (5) represent the energy percentage of both tidal and non-tidal.

$$\text{TP \%} = \frac{\text{MTP}}{(\text{MTP} + \text{MRP})} X\ 100 \qquad (4)$$

$$\text{RP \%} = \frac{\text{MRP}}{(\text{MRP} + \text{MTP})} X\ 100 \qquad (5)$$

Where TP is the tidal power percentage, RP is the residual power percentage, MTP is the mean tidal power, and MRP is the mean residual power.

3. RESULTS AND DISCUSSION

3.1. Harmonic analysis

For the available observed sea-level data, using Delft-3D tide-suit and harmonic analysis technique as mentioned before, it is identified by the algorithm of tide suit that there are 11 significant tidal constituents dominating the signal (Figures 5a – 5b), showing the results of harmonic analysis of both tidal and non-tidal components after being separated.
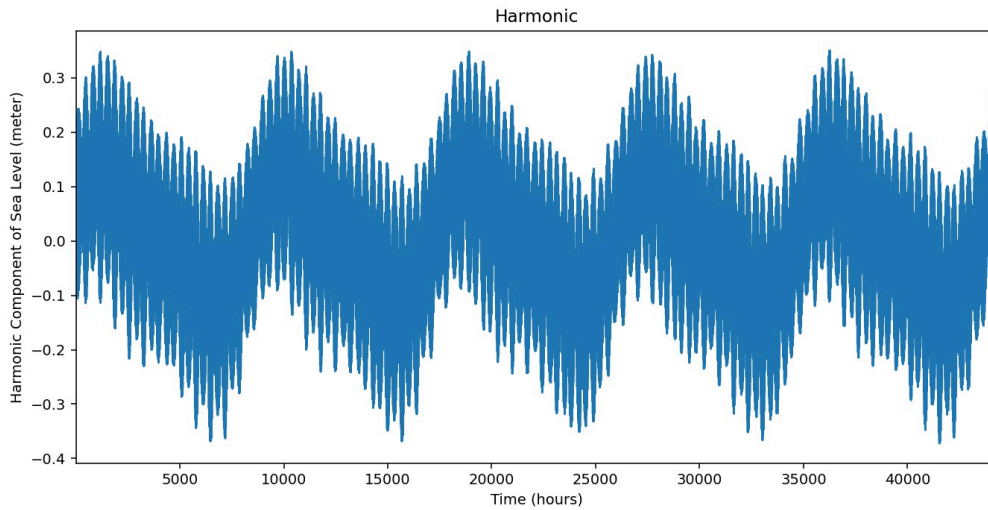
Figure 5a. Harmonic signal of available observed sea-level data set after being analyzed by Delft-3D tide suit and illustrated using MATLAB
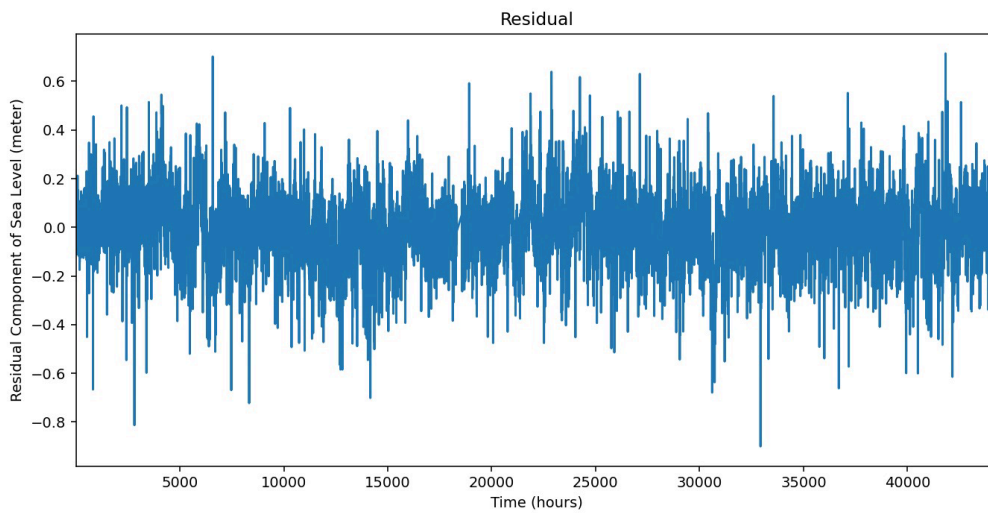
Figure 5b. Residual signal of available observed sea-level data set after being analyzed by Delft-3D tide suit and illustrated using MATLAB

Tidal constituents	Amplitude (CM)	Phase deg.	Tidal constituents	Amplitude (CM)	Phase deg.
*M2	11.23	234.86	*K2	1.86	331.04
*SA	10.41	242.52	*O1	1.65	26.8
*S2	6.85	308.64	*S1	1.4	121.38
*SSA	3.5	249.32	*MM	1.38	255.18
*K2	2.19	311.7			
*K1	2.17	121.42			
*N2	1.86	205.83			

Table 1. The most significant tidal components (Amplitudes and Phases (GMT+2))

It is obvious that the largest constituent in amplitude is M2 with 11.23 cm with phase angle 234.86°, while the smallest value is MM with 1.38 cm with phase angle 255.18°.

Period	Period from 01/01/2015 to 31/12/2015 (Radwan et al., 2021)		Period from 23/6/2010 to 14/07/2015	
Constituents	Amplitude (cm)	Phase (degree)	Amplitude (cm)	Phase (degree)
M2	11.32	336.483	11.23	234.86
S2	6.694	308.189	6.85	308.64
K1	1.751	295.205	2.17	121.42
O1	1.453	309.215	1.65	26.8
P1	1.244	238.207	0.68	121.72
N2	1.945	64.742	1.86	205.83
K2	1.147	295.553	2.19	311.7
Q1	0.367	112.845	0.19	345.77
M4	0.17	240.842	0.12	300.76

Table 2. Comparison of results obtained with previous studies

The obtained results were compared by the results obtained by (Radwan et al., 2021) which showed an accurate similarity between the most significant semidiurnal constituents amplitudes with no difference in M2 and a difference in S2 by 0.16 cm, the diurnal constituents shown less accuracy with larger differences, the big differences in phase is due to the location sensor, the different period of time used by the two studies, and different number of tidal constituents used in Delft 3D than T-Tide software as it used only 10 tidal constituents in the analysis while Delft3D used 71 tidal constituents.

3.2. Correlation to meteorological conditions

The analysis aimed to determine the correlation between the surge component and the wind vector. The results presented in Table 3 indicate a weak correlation between the surge component and the wind vector, whether in the X and Y directions or normal and parallel to the coast. This weak correlation can be attributed to local topographic features and the lag effect of wind on the surge. The lag effect refers to the time it takes for the impact of wind on sea level variation to become evident. Therefore, it was necessary to explore additional factors that influence sea level, considering that other variables may play a more significant role in the sea-level variations.

	Annual correlation of surge with:			
YEAR	Wind in dr. x	Wind in dr. y	Wind normal to coast	Wind parallel to coast
2010	-0.18	-0.26	-0.03	0.32
2011	-0.32	-0.02	-0.28	0.20
2012	-0.29	-0.08	-0.23	0.22
2013	-0.25	-0.03	-0.20	0.17
2014	-0.23	0.03	-0.21	0.12
2015	-0.40	0.00	-0.37	0.24

Table 3. Results of correlation between surge and meteorological component wind vector

Based on the correlation analysis, it was observed that there is a weak correlation between the surge component and temperature (T) as well as atmospheric pressure (P). Despite the weak correlation, there is still a discernible trend in sea-level rise (SLR) from 2011 to 2015, with an approximate rate of 2 mm/year. This

suggests that other factors beyond temperature and atmospheric pressure may be contributing to the observed surge elevation and subsequent rise in sea level during this period, such as local hydrodynamics, wave activity, and coastal morphology. Interestingly, the surge component was found to have an inverse proportionality with atmospheric pressure, meaning that lower atmospheric pressure was associated with a rise in the sea level. This inverse relationship contributes to the overall trend of sea-level rise during the study period. However, in 2010, a different pattern was observed, with a downward trend line in the sea level at a rate of 0.3 mm/year. Despite the weak correlation between meteorological parameters and surge components, this downward trend indicates that other factors may be influencing sea level variations during that specific year.

	Annual correlation of surge with:	
YEAR	temperature	pressure
2010	-0.47	0.16
2011	0.11	-0.39
2012	0.03	-0.16
2013	-0.14	-0.21
2014	0.05	-0.24
2015.00	-0.07	-0.30

Table 4. Results of correlation between surge and meteorological components

Sea level was correlated annually with meteorological parameters to represent one complete cycle of annual meteorological parameters effect on Sea level rise from 2011 to the end of June 2015. The tide gauge station showed a small rate of sea level rise. This observation suggests that the station was highly protected from the direct impact of meteorological effects during this period. The correlation analysis, as presented in Table 4, indicates a proportional relationship between sea level and temperature, as well as atmospheric pressure, within this time frame. However, it is important to note that 2010 exhibited a different pattern. During this year, there was an inverse correlation between sea level and temperature, indicating that higher temperatures were associated with lower sea levels. Additionally, there was a direct correlation between sea level and atmospheric pressure, suggesting that higher atmospheric pressure corresponded to higher sea levels. This anomalous behavior in 2010 may be attributed to specific meteorological conditions or local factors that deviated from the overall pattern observed in other years.

3.3. Form factor

Using Eq. (1) for Form Factor and the amplitudes of the four major dominant constituents (O1, K1, M2, and S2), 1.65, 2.17, 11.23, 6.85 respectively are shown in Table 2. Form Factor shows that the tide in the study area is semidiurnal, where FF equals 0.21. The most significant tidal constituents are the semidiurnal components M2 and S2, with amplitudes equal to 11.23 and 6.85 cm respectively.

3.4. Tide asymmetry

Using Eq. (2) and (3) for judgement of the flow in the study area after harmonic constituent analysis, with values of both amplitudes and phases of M2, M4 presented in Table 2, which represents the dominant constituents in the sediment transport. Using Eq. (4), it was found that the amplitude ratio for simulated and observed constituents was 0.0193, 0.0191 respectively. Using Eq. (5) by the given phase shows that $180° < ØM4 < 360°$. The amplitude ratio of M4 over M2 was computed to be 0.01068 > 0.01, which reflects a tide wave distortion, while ØM4 was found to be in between 0° to 180°. According to the above mentioned, it is flood-dominant with short flood period.

3.5. Power spectral density

Spectral analysis was applied to get the spectral estimates before and after the removal of tidal energy. It is also used to decompose the time series into different significant harmonic components, each of them associated with a significant frequency. A measure for the power of each frequency is expressed by the value of the spectrum as shown in Figure 6.
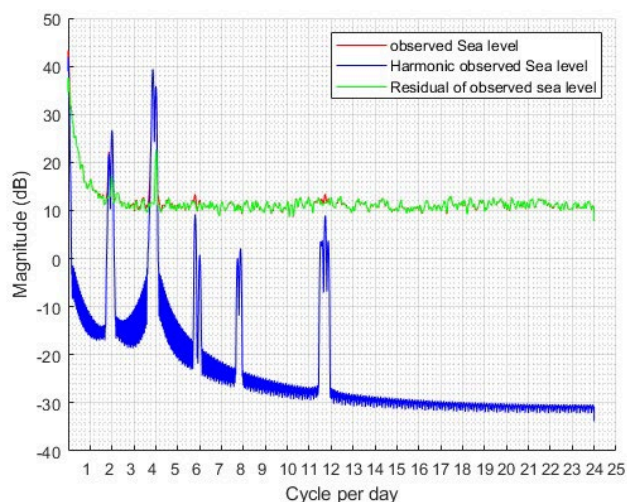

Figure 6. Power spectral density (PSD) of observed sea level data with both tidal and non-tidal components measured in Port Said from 23 June 2010 to 14 July 2015

A very significant and obvious contribution of solar annual tidal constituent (Sa) and solar semi-annual tidal constituent (Ssa) by 10.41 cm – 3.5 cm amplitudes and 242° – 249.31° phase angle respectively, which refers to the activity of the Sun, where only the data exceeds 6 months or a year, and account for the non-uniform changes of the Sun declination and distance. Coinciding with a contribution to the signal power by the semidiurnal tidal constituents (M2) is the principal lunar semidiurnal constituent, and S2 is the principal solar semidiurnal constituent by 11.32 cm with phase 234.86° and 6.85 cm and 308.64° for the phase.

3.6. Residual and tidal energy percentage

Using a MATLAB code in Eq. (4), (5) calculation for the determination of tidal and non-tidal power percentage, which means the energy contribution of each component in the original signal, it is shown in Table 5 that both components have almost the same effect.

Components	Power percentages of observed sea level
Residual power	49.37%
Tidal power	50.63%

Table 5. Results of energy percentage for both (tidal – non-tidal) components

From Table 5, it is clear that the sea-level change is controlled by the significant tidal constituents and the storm surge due to the non-tidal components almost by an equal percentage.

4. CONCLUSION

Based on the analysis of sea level harmonics, the prominent tidal constituents in the study area are the semidiurnal components (M2, S2), along with the solar annual (Sa) and solar semi-annual (Ssa) constituents, which can be attributed to meteorological effects.

The tidal regime in the study area is classified as semidiurnal, with a ratio of 0.21 based on the FF ratio computations. The sea level trend is influenced by the correlation of surge components with meteorological parameters such as wind vector, temperature, and atmospheric pressure. This correlation shows a weak direct correlation with surge, resulting in a low rate of sea level rise except for 2010, when a negative trend line was observed due to an inverse moderate correlation with temperature (-0.47) and a weak direct correlation with atmospheric pressure (0.16).

The interactions between M2 and M4 indicate a considerable distortion in the tidal wave, as indicated by (Ar.) > 0.01. Additionally, the phase difference between M2 and M4 suggests that the harbor system experiences a dominance of short-period flood. Spectral analysis reveals that the energy percentage of the tidal component, mainly contributed by the solar annual, solar semiannual, M2, and S2 constituents, accounts for most of the spectral energy at the sea level. The residual signal also contributes significantly to the original sea-level signal.

The effect of the sea level rise on the study area is meeting the global rate, which makes the area of Port Said susceptible to serious flooding. Therefore, developing appropriate adaptation strategies in coastal areas must be considered.

4.1. Recommendation for future work

1) Further investigate the relationship between meteorological parameters and surge components to better understand their influence on sea-level rise.
2) Explore the causes of tidal-wave distortion and its implications for coastal areas.
3) Conduct long-term monitoring and analysis to assess any changes in tidal characteristics and sea level trends.
4) Investigate the impact of other factors, such as wave activity and coastal morphology, on the sea level variations in the study area.

CONFLICT OF INTEREST

The authors declare no conflict of interest.

REFERENCES

Biton, E. 2020, 'Possible implications of sea level changes for species migration through the Suez Canal', Scientific Reports, 10(1), pp. 1-16.

Cazenave, A., Cabanes, C., Dominh, K. & Mangiarotti, S. 2001, 'Recent sea level change in the Mediterranean Sea revealed by Topex/Poseidon satellite altimetry', Geophysical Research Letters, 28(8), pp. 1607-1610.

Dias, J.M., Valentim, J.M. & Sousa, M.C. 2013, 'A numerical study of local variations in tidal regime of Tagus estuary, Portugal', PLoS ONE, 8(12), e80450.

El-Fishawi, N.M. 1993, 'Recent sea level changes and their implications along the Nile delta coast', in International workshop on sea level changes and their consequences for hydrology and water management, [details of publication if available].

El-Geziry, T. & Radwan, A. 2012, 'Sea level analysis off Alexandria, Egypt', Egyptian Journal of Aquatic Research, 38, pp. 1–5.

El-Geziry, T.M. & Said, M.A. 2019, 'Sea level variations in El-Burullus new harbour, Egypt', Arabian Journal of Geosciences, 12, p. 460.

El-Geziry, T.M. & Said, M.A. 2020, 'Spatial variations of sea level along the Egyptian Mediterranean Coast', Athens Journal of Mediterranean Studies, 6(2), pp. 141–154.

El-Geziry, T.M. 2020, 'On the vulnerability of the Egyptian Mediterranean Coast to the sea level rise', Athens Journal of Sciences, 7(4), pp. 195–206.

Hendy, D.M., El-Geziry, T.M., El Raey, M. & Nasr, S.M. 2021, 'Sea level characteristics and extremes along Alexandria coastal zone', Arabian Journal of Geosciences, 14, p. 1273.

IPCC 2014, Climate change 2014 synthesis report, IPCC, Geneva, Switzerland, pp. 1059-1072.

Mackie, J.A., Rowlatt, M. & Reimer, M.J. 2021, 'Alexandria', Encyclopedia Britannica, September 28, available at: https://www.britannica.com/place/Alexandria-Egypt.

Pawlowicz, R., Beardsley, B. & Lentz, S. 2002, 'Classical tidal harmonic analysis including error estimates in MATLAB using T_TIDE', Computers & Geosciences, 28(8), pp. 929-937.

Pugh, D. 2004, Changing sea levels: effects of tides, weather and climate, Cambridge University Press.

Pugh, D.T. 1987, Tides, surges and mean sea level, [publisher information if available].

Radwan, A.M., Magdy, M., Rabah, M., Saber, A. & Zaki, A. 2021, 'Sea level analysis using tide gauge observations at the northern delta coast, Egypt', NRIAG Journal of Astronomy and Geophysics, 10(1), pp. 361-371.

Riding, J. & Rawson, A. 2015, 'South-West Pacific Regional Hydrography Program: LINZ Hydrography Risk Assessment Methodology', Land Information New Zealand, Wellington, New Zealand.

Sharaf El Din, S.H., Khafagy, A.M., Fanos, A.M. & Ibrahim, A.M. 1989, 'Extreme sea level values on the Egyptian Mediterranean coast for the next 50 years', in International Seminar on Climatic Fluctuations and Water Management, Cairo, p. 15.

Stark, J., Smolders, S., Meire, P. & Temmerman, S. 2017, 'Impact of intertidal area characteristics on estuarine tidal hydrodynamics: A modelling study for the Scheldt Estuary', Estuarine, Coastal and Shelf Science, 198, pp. 138-155.

Syvitski, J.P.M., Kettner, A.J., Overeem, I., Hutton, E.W.H., Hannon, M.T., Brakenridge, G.R., ... Nicholls, R.J. 2009, 'Sinking deltas due to human activities', Nature Geoscience, 2, pp. 681–686.

Tetra Tech 1984, Shoreline master plan for the Nile Delta coast: Progress Report 1, Tetra Tech, Pasadena, California, p. 143.

Tonbol, K. & Shaltout, M. 2013, 'Tidal and non-tidal sea level off Port Said, Nile Delta, Egypt', JKAU: Marine Sciences, 24(2), pp. 69-83.

Tsimplis, M.N. & Rixen, M. 2002, 'Sea level in the Mediterranean Sea: The contribution of temperature and salinity changes', Geophysical Research Letters, 29(23), pp. 51-1.

Tsimplis, M.N., Proctor, R. & Flather, R.A. 1995, 'A two-dimensional tidal model for the Mediterranean Sea', Journal of Geophysical Research, 100(C8), pp. 16223–16239.